GASTROINTESTINAL

Can IVIM help predict HCC recurrence after hepatectomy?

Yao Zhang[1] · Sichi Kuang[1] · Qungang Shan[1] · Dailin Rong[1] · Zhongping Zhang[2] · Hao Yang[1] · Jun Wu[1] ·
Jingbiao Chen[1] · Bingjun He[1] · Ying Deng[1] · Neil Roberts[3] · Jun Shen[4] · Sudhakar K. Venkatesh[5] · Jin Wang[1]

Abstract

Purpose To determine the diagnostic performance of intravoxel incoherent motion (IVIM) parameters to predict tumor recurrence after hepatectomy in patients with hepatitis B virus (HBV)–related hepatocellular carcinoma (HCC).

Materials and methods One hundred and fifty-seven patients (mean age 52.54 ± 11.32 years, 87% male) with surgically and pathologically confirmed HCC were included. Regions of interests were drawn including the tumors by two independent radiologists. ADC and IVIM-derived parameters (true diffusion coefficient [D]; pseudodiffusion coefficient [D^*]; pseudodiffusion fraction [f]) were obtained preoperatively. The Cox proportional hazards model was used to analyze the predictors associated with tumor recurrence after hepatectomy.

Results Forty-seven of 157 (29.9%) patients experienced tumor recurrence. The multivariate Cox proportional hazards model revealed that a D value $< 0.985 \times 10^{-3}$ mm^2/s (hazard ratio (HR), 0.190; $p = 0.023$) was a risk factor for tumor recurrence. Additional risk factors included younger age (HR, 0.328; $p = 0.034$) and higher serum alpha-fetoprotein (AFP) level (HR, 2.079; $p = 0.013$). Further, receiver operating characteristic (ROC) analysis showed that the area under the curve (AUC) of the obtained Cox regression model improved from 0.68 for the combination of AFP and age alone to 0.724 for the combination of D value, AFP, and age.

Conclusion The D value derived from the IVIM model is a potential biomarker for the preoperative prediction of recurrence after hepatectomy in patients with HCC. When combined with age and AFP levels, D can improve the predictive performance for tumor recurrence.

Key Points
- *The recurrence rate of HCC after hepatectomy was higher in patients with ADC, D, and f values that were lower than the optimal cutoff values.*
- *The optimal cutoff values of ADC, D, D*, and f for predicting recurrence in HBV associated HCC were 0.858×10^{-3} mm^2/s, 0.985×10^{-3} mm^2/s, 12.5×10^{-3} mm^2/s, and 23.4%, respectively.*
- *The D value derived from IVIM diffusion-weighted imaging may be a useful biomarker for preoperative prediction of recurrence after hepatectomy in patients with HCC. When combined with age and AFP levels, D can improve the predictive performance for tumor recurrence.*

Yao Zhang and Sichi Kuang contributed equally to this work.

Electronic supplementary material The online version of this article (https://doi.org/10.1007/s00330-019-06180-1) contains supplementary material, which is available to authorized users.

✉ Jin Wang
wangjin3@mail.sysu.edu.cn

1 Department of Radiology, the Third Affiliated Hospital, Sun Yat-sen University (SYSU), No 600, Tianhe Road, Guangzhou 510630, People's Republic of China

2 Philips Intergrated Solution Center, Guangzhou, People's Republic of China

3 Edinburgh Imaging, School of Clinical Sciences, University of Edinburgh, Edinburgh EH16 4TJ, UK

4 Department of Radiology, Sun Yat-sen Memorial Hospital, Sun Yat-sen University (SYSU), No 107, Yanjiang Road, West, Guangzhou 510120, People's Republic of China

5 Department of Radiology, Mayo Clinic College of Medicine, Mayo Clinic, 200 First Street SW, Rochester, MN 55905, USA

Abbreviations

ADC	Apparent diffusion coefficient
AFP	Alpha-fetoprotein
AUC	Area under the curve
CI	Confidence interval
D	True diffusion coefficient
$D*$	Pseudodiffusion coefficient
f	Pseudodiffusion fraction
HBP	Hepatobiliary phase
HBV	Hepatitis B virus
HCC	Hepatocellular carcinoma
HR	Hazard ratio
ICC	Intra-class correlation coefficient
IVIM	Intravoxel incoherent motion
ROC	Receiver operating characteristic
T2WI	T2-weighted imaging

Introduction

Hepatocellular carcinoma (HCC) is the most common primary malignancy of the liver and is a major cause of mortality [1, 2]. Despite considerable advances in early diagnosis and surgical techniques, and improved post-operative management, the tumor recurrence rate remains high (50–60%) after curative resection [3, 4]. Studies have shown that microvascular invasion, poor histologic differentiation, and microsatellite nodules are more likely to be associated with recurrence after hepatic resection [5, 6]. Most of these risk factors, however, can only be assessed at post-operative pathologic examination and are therefore of limited value in guiding treatment decisions prior to hepatic resection.

Recently, preoperative imaging features such as rim enhancement and arterial peritumoral enhancement on dynamic contrast-enhanced magnetic resonance imaging (MRI) [7, 8], as well as non-smooth tumor margins [9], and tumor size [10] have proven useful for predicting HCC recurrence. Other imaging features, such as HCC capsule and hypointense nodules in the hepatobiliary phase (HBP) on hepatobiliary contrast agent-enhanced MRI, have also been proposed for predicting tumor behavior [11, 12]. Most of these imaging indices, however, are qualitative measurements and therefore subject to interpreter bias, possibly resulting in low diagnostic performance in predicting tumor recurrence after hepatectomy.

Diffusion-weighted imaging (DWI) can quantitatively evaluate the apparent mobility of water molecules in tissues, as indicated by the apparent diffusion coefficient (ADC) [13]. Previous studies have shown that low ADC values derived from DWI can be used to evaluate tumor behavior and recurrence after hepatectomy in patients with HCC [14–16]. However, because ADC values reflect a combination of diffusion and blood perfusion effects, they may not entirely account for all tissue characteristics [17, 18]. Conversely, intravoxel incoherent motion (IVIM) values derived from DWI with multiple b value models can reflect tissue diffusion and microcapillary perfusion separately [19]. A recent study has suggested that IVIM parameters correlate well with the degree of HCC differentiation [20]. The aim of our study was to determine whether IVIM values can be used to predict tumor recurrence in patients with HCC after curative resection.

Materials and methods

Patients

This retrospective study followed the principles of the Declaration of Helsinki and was approved by the Institutional Review Board. Written informed consent was waived. Between 1 March 2014 and 31 July 2017, all patients referred for abdominal MRI for suspected HCC due to chronic hepatitis B virus (HBV) infection were evaluated. Patients were ineligible for inclusion if they (a) had a tumor other than HCC, (b) had undergone previous anti-tumor treatment, (c) underwent hepatectomy at > 1 month after the MRI examination, (d) had simultaneous hepatitis C virus infection or any other chronic hepatic diseases carrying the risk of cirrhosis, (e) a lesion size < 1 cm, (f) massive necrosis and hemorrhage that could potentially impact accurate measurement, (g) obvious slice misregistration or motion artifacts, (h) no or irregular anti-HBV-DNA treatment after hepatectomy, (i) were unavailable or lost to follow-up, and (j) had a tumor with macrovascular invasion, which was defined as gross invasion into the main portal veins or their branches, hepatic veins or the inferior vena cava at gross examination or at imaging including MRI and computed tomography (CT), because such tumors are known to have a greater risk of recurrence [21–24] (Fig. 1).

Clinical information, laboratory data, and pathology reports of eligible patients were retrospectively retrieved from our database. All patients were treated by curative resection, which was defined as complete macroscopic removal of the tumor with ample free section margins. The median time between the MRI examination and surgery was 7 days (range, 1–14 days).

Post-operative follow-up in all of the study patients after curative resection for HCC was performed with abdominal

ultrasound and either contrast-enhanced CT or MRI, initially at 3-month intervals during the first year, and thereafter at 6-month intervals. In addition, serum liver profiles (alpha-fetoprotein [AFP] and HBV DNA levels) were obtained. Tumor recurrence was suspected when the serum AFP levels were progressively elevated and ultrasonography revealed a new hepatic lesion. Recurrence was diagnosed by dynamic CT ($n = 15$) or MRI ($n = 32$) according to typical imaging characteristics (hyper-enhancement on arterial phase images and washout on portal venous and/or delayed-phase images) [25, 26]. Recurrence was confirmed by surgical pathology when patients underwent re-resection ($n = 8$) or with biopsy ($n = 5$). All patients were followed until December 2017. The mean

and median follow-up times for surviving patients after hepatic resection were 15 and 14 months (range, 3–43 months), respectively.

MRI protocol

MRI investigations were performed on a 3.0 T scanner (Discovery MR750; GE Healthcare) equipped with an eight-channel phased-array abdominal coil. All patients had fasted for at least 4 h before examination. DWI was performed by using a respiratory-triggered single-shot spin echo echo-planar imaging sequence in the transverse plane before contrast-enhanced imaging. Eleven b values from 0 to 1500 s/mm^2 (0, 30, 50, 100, 150, 200, 300, 500, 800, 1000, and 1500) were applied and the number of excitations (NEX) for each b value was 1, 1, 1, 1, 1, 1, 2, 4, 4, 6, and 6, respectively. The acquisition parameters of the multiple b value DWI sequences were as follows: repetition time = 6000 to 10,000 ms, echo time = 56 ms, bandwidth = 250 kHz/pixel, acquisition matrix = 128 × 128, field of view = 38 × 30 cm, slice thickness = 5 mm, and slice gap = 1 mm. The acquisition of the DWI sequence with multiple b values typically took between 4 and 7 mins. The three perpendicular x, y, z gradient directions were applied simultaneously (i.e., 3-in-1 option on GEHC system). Gadobenate dimeglumine (MultiHance; Bracco) was administered intravenously using a dual-head power-injected bolus injector (Spectris Solaris EP; Medrad) at a dose of 0.1 mmol/kg bodyweight and at a flow rate 2.0 mL/s, followed by a 20-mL saline flush at the same rate. The liver protocols and the detailed acquisition parameters of the other MRI sequences used are summarized in Table 1.

IVIM post-processing and analysis

The ADC values were estimated by fitting diffusion-weighted signals at all b values (0–1500 s/mm^2) to the following mono-exponential equation:

$$S_b/S_0 = \exp(-b \cdot \text{ADC})$$

where S_b is the signal intensity at a given b value and S_0 is the signal intensity without diffusion weighting.

The IVIM model uses a bi-exponential fitting of the diffusion decay curve to separate true diffusion from "pseudodiffusion" which reflects tissue microperfusion. In the IVIM model, the signal intensity curves from a DWI acquisition with multiple b values are described by Eq. [1] as follows [19]:

$$S_b/S_0 = (1-f) \cdot \exp(-b \cdot D) + f \cdot (-b \cdot D^*) \tag{1}$$

where S_b and S_0 are signal intensities with and without diffusion weighting, respectively, D (true diffusion coefficient) represents pure molecular diffusion, D^* (pseudodiffusion
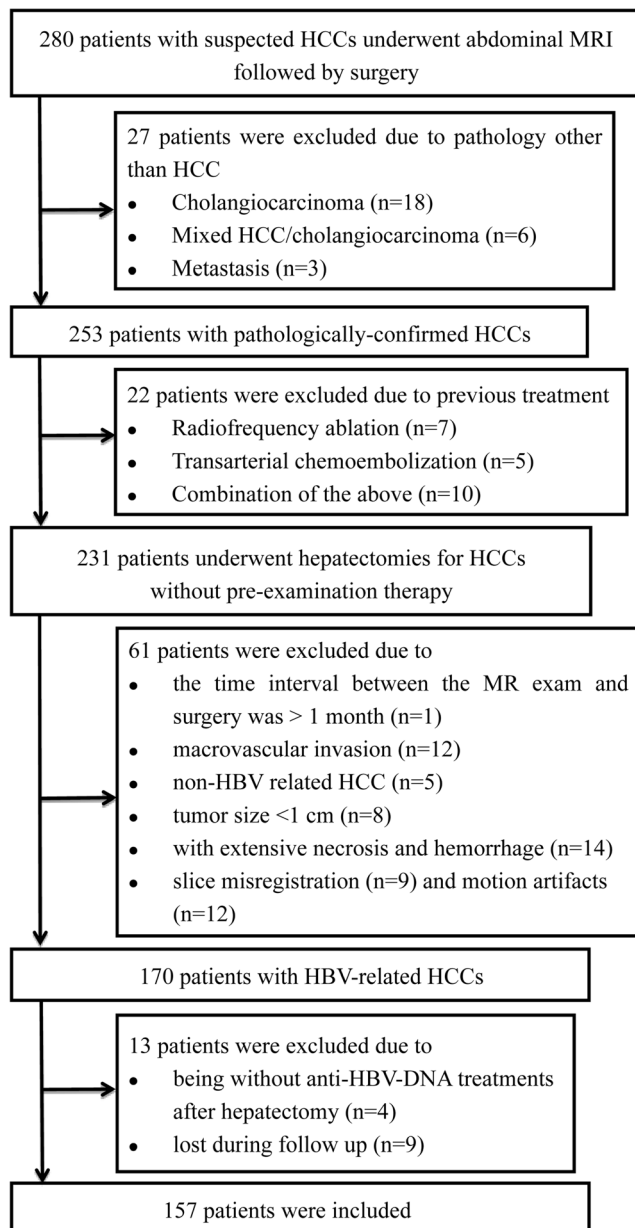

Fig. 1 Flowchart of inclusion and exclusion criteria. HCC, hepatocellular carcinoma; MRI, magnetic resonance imaging; HBV, hepatitis B virus

The flowchart contains the following boxes:

280 patients with suspected HCCs underwent abdominal MRI followed by surgery

27 patients were excluded due to pathology other than HCC
- Cholangiocarcinoma (n=18)
- Mixed HCC/cholangiocarcinoma (n=6)
- Metastasis (n=3)

253 patients with pathologically-confirmed HCCs

22 patients were excluded due to previous treatment
- Radiofrequency ablation (n=7)
- Transarterial chemoembolization (n=5)
- Combination of the above (n=10)

231 patients underwent hepatectomies for HCCs without pre-examination therapy

61 patients were excluded due to
- the time interval between the MR exam and surgery was > 1 month (n=1)
- macrovascular invasion (n=12)
- non-HBV related HCC (n=5)
- tumor size <1 cm (n=8)
- with extensive necrosis and hemorrhage (n=14)
- slice misregistration (n=9) and motion artifacts (n=12)

170 patients with HBV-related HCCs

13 patients were excluded due to
- being without anti-HBV-DNA treatments after hepatectomy (n=4)
- lost during follow up (n=9)

157 patients were included

Table 1 MRI acquisition parameters

Sequence	Matrix	TR /TE (ms)	Flip angle (degree)	Field of view (cm)	Bandwidth (kHz)	Slice thickness (mm)	Slice gap (mm)	Acquisition time
FIESTA	224 × 256	3.1/1.1	45	38 × 38	125	8	1	10 s
SSFSE	384 × 160	1222/80.9	90	44 × 44	83.3	8	0	21 s
T2WI	320 × 320	6000/72.8	110	36 × 36	83.3	5	1	3 min 36 s
DW single-shot EPI	128 × 128	6000–10,000/56	90	38 × 30	250	5	1	4–7 min
LAVA-Flex pre-contrast	260 × 224	3.7/1.7	15	36 × 36	200	5	1	14 s
LAVA-Flex dynamic*	260 × 224	3.7/1.7	12	36 × 36	200	5	1	–

Repetition time of IVIM is automatically calculated on the basis of the respiratory rate and respiratory interval number

FIESTA fast imaging employing steady-state acquisition, *SSFSE* single-shot fast spin echo, *DW* diffusion-weighted, *EPI* echo-planar imaging, *LAVA* liver acquisitions with volume acceleration, *TR* repetition time, *TE* echo time

*After the contrast-medium injection, arterial phase, portal venous phase, and delayed-phase imaging were subsequently acquired at 15–20 s, 60 s, and 180 s, respectively

coefficient) represents incoherent microcirculation within the voxel, and *f* (pseudodiffusion fraction) is the proportion of the pseudodiffusion. To robustly separate the diffusion and perfusion effects in Eq. [1], a typical multi-step approach is applied [27–29]. Initially, *D* is estimated by mono-exponential fitting of the diffusion-weighted signals at high *b* values ($b > 200$ s/mm^2) assuming that perfusion contributions are negligible in Eq. [2].

$$S_b/S_0 = \exp(-b \cdot D) \qquad (2)$$

The pseudodiffusion fraction *f* and pseudodiffusion coefficient *D** are subsequently estimated by fitting the measured signal intensity at all *b* values to Eq. [1] with fixed *D*.

Image analysis was performed independently by two abdominal imaging radiologists (S.K. with 14 years and Y.Z. with 3 years of experience in liver MRI), who were blinded to all clinical, laboratory, pathologic, and follow-up information. The workstation with FuncTool software (version AW 4.6, GE Healthcare) was used for post-processing. The region of interest (ROI) was manually drawn to encompass as much of the lesion as possible in the maximum tumor cross-section on a single axial ($b = 1000$ s/mm^2) image using T2-weighted imaging (T2WI) as a reference, after reviewing all T2WI, DWI, and dynamic enhancement images. ROI boundaries were placed at least 5 mm away from the margin of the lesion to avoid partial volume effects [30]. Regions of necrosis and hemorrhage were avoided using the T2WI and dynamic enhancement on the T1-weighted images as reference. Subsequently, the IVIM parameters were calculated automatically. The final value of each parameter was the average of the values measured by the two radiologists. Additionally, the respective measures obtained by the two radiologists were used to determine inter-observer agreement expressed in terms of the intra-class correlation coefficient (ICC). A third abdominal imaging radiologist (H.Y. with 3 years of experience in

liver MRI) performed an analysis of tumor size by measuring the longest cross-sectional diameter on axial images according to the liver imaging reporting and data system, version 2017 [31]. In patients with multiple tumors, a target tumor with the longest cross-section was selected for analysis.

Statistical analysis

Data for continuous measures are reported as the mean ± standard deviation or as the median and range when the two-sample *t* tests or nonparametric Mann–Whitney tests were used. Categorical variables are presented as numbers of patients and percentages and were analyzed by means of the chi-square or Fisher's exact test. The best cutoff value for each IVIM-derived parameter was determined based on receiver operating characteristic (ROC) curves. Inter-observer agreement in measuring the IVIM values was determined by means of the ICC with 95% confidence interval (CI) and was interpreted as follows: 0.00–0.20, poor correlation; 0.21–0.40, fair correlation; 0.41–0.60, moderate correlation; 0.61–0.80, good correlation; and 0.81–1.00, excellent correlation [32, 33]. The follow-up time was calculated from the date of resection to the date when tumor recurrence was diagnosed, or from the date of the resection to the last visit if recurrence was not diagnosed and the patients were censored on the date of death or on the last date of follow-up. Recurrence-free survival rates were computed using the Kaplan–Meier method and compared using the log-rank test. Univariate analysis was performed to assess significant clinical characteristics and IVIM values associated with tumor recurrence after curative resection. Multivariate Cox regression (stepwise forward model) analysis was performed to identify independent predictors of recurrence. The results are expressed as hazard ratios (HRs) with 95% CIs. Finally, ROC curve analysis was used to evaluate the obtained multivariate Cox regression model. All

statistical analyses were performed using SPSS 22.0 (IBM). $p < 0.05$ was considered statistically significant.

Results

Study population

The characteristics of the patients evaluated in this study are summarized in Table 2. Overall, tumor recurrence after hepatectomy occurred in 47 (29.9%) of the 157 patients included in the analysis. In 13/47 patients, recurrence was confirmed by biopsy ($n = 5$) or by pathologic assessment after re-resection ($n = 8$). In the remaining, the recurrence was diagnosed on follow-up CT ($n = 8$), MR ($n = 21$), and both CT and MRI ($n = 5$). The median time from hepatectomy to HCC recurrence was 14 months (range 4–32 months). The principal sites of recurrence were the distal segment ($n = 21$ [45%]), the adjacent segment ($n = 15$ [32%]), and the marginal segment ($n = 3$ [6%]). In eight patients [17%], recurrence was multisegmental. The median longest cross-section of largest recurrent tumor was 17 mm (range 5–47 mm).

Comparison of clinical and pathologic characteristics according to IVIM values

The inter-observer agreement was very good for ADC (ICC = 0.896, 95% CI = 0.841–0.932), D (ICC = 0.889, 95% CI = 0.831–0.927), and f (ICC = 0.870, 95% CI = 0.803–0.915). Moderate inter-observer agreement was observed for D^* (ICC = 0.600, 95% CI = 0.437–0.725). ROC analysis showed that the optimal cutoff values for ADC, D, D^*, and f for predicting recurrence were 0.858×10^{-3} mm²/s, 0.985×10^{-3} mm²/s, 12.5×10^{-3} mm²/s, and 23.4%, respectively.

The patients were divided into two groups with optimal cutoff value for each of the IVIM metrics for predicting recurrence. The clinical and pathological characteristics of the two groups were then compared based on optimal cutoff value for each of the IVIM metrics (Table 3). Patients with ADC values $\leq 0.858 \times 10^{-3}$ mm²/s tended to have higher serum AFP levels than those patients with ADC values $> 0.858 \times 10^{-3}$ mm²/s (30 [48%] vs 25 [27%], $p = 0.007$). Furthermore, there were more well-differentiated HCC lesions in patients with ADC levels $> 0.858 \times 10^{-3}$ mm²/s (38 [40%]), D values $> 0.985 \times 10^{-3}$ mm²/s (15 [65%]), and f values $> 23.4\%$ (22 [41%]) than in patients with ADC values $\leq 0.858 \times 10^{-3}$ mm²/s (2 [2%]), D values $\leq 0.985 \times 10^{-3}$ mm²/s (25 [19%]), and f values $\leq 23.4\%$ (18 [17%]) ($p < 0.001$–0.001). Finally, HCC lesions with f values $\leq 23.4\%$ more frequently demonstrated microvascular invasion (51 [50%] vs 16 [30%], respectively, $p = 0.017$). No significant differences in

Table 2 Demographic and clinical characteristics of the 157 patients with HCCs

Characteristics	All patients ($n = 157$)
Demographics	
Age, year	52.54 (± 11.32)
Sex	
Male	137 (87%)
Female	20 (13%)
BMI* (kg/m²)	23 (15–32)
Biochemical profile	
AST level*, IU/L	31 (13–176)
ALT level*, IU/L	35 (12–168)
AST/ALT*	0.95 (0.36–3.50)
TBIL*, mg/dL	13 (3.20–134.70)
HBV DNA*, ×10⁵ IU/mL	0.0416 (0–1300)
AFP*, ng/mL	44.06 (1–121,000)
NLR*	1.79 (0.73–19.04)
Radiological characteristics	
Number of tumors	
Single	108 (69%)
Multiple	49 (31%)
Tumor size, mm	36 (14–112)
Tumor size group	
< 50 mm	111 (71%)
≥ 50 mm	46 (29%)
Child-Pugh	
A	151 (96%)
B	6 (4%)
Histological characteristics	
Differentiation	
Well	40 (25%)
Moderate and poor	117 (75%)
Capsule	
Absent	45 (29%)
Present	112 (71%)
Microvascular invasion	
Absent	90 (57%)
Present	67 (43%)
Recurrence	47 (29.94%)

Note: Unless otherwise indicated, data are the mean and standard deviation (SD) or numbers with percentages in parentheses

AST aspartate aminotransferase, *ALT* alanine aminotransferase, *TBIL* total bilirubin, *HBV* hepatitis B virus, *AFP* α-fetoprotein, *NLR* neutrophil to lymphocyte ratio

*Presented as the median and range

baseline clinical or pathological characteristics were observed between groups with $D^* \leq 12.5 \times 10^{-3}$ mm²/s and $D^* > 12.5 \times 10^{-3}$ mm²/s ($p > 0.05$ for all variables).

Table 3 Patient demographic data and comparison of the patient characteristics according to the IVIM metrics

Characteristics	ADC (×10⁻³ mm²/s)			D (×10⁻³ mm²/s)			D* (×10⁻³ mm²/s)			f (%)		
	> 0.858 (n = 94)	≤ 0.858 (n = 63)	p value	> 0.985 (n = 23)	≤ 0.985 (n = 134)	p value	> 12.5 (n = 66)	≤ 12.5 (n = 91)	p value	> 23.4 (n = 54)	≤ 23.4 (n = 103)	p value
Age > 60 years	24 (26%)	12 (19%)	0.342	5 (22%)	31 (23%)	0.883	15 (23%)	21 (23%)	0.959	16 (30%)	20 (19%)	0.148
Sex Male	86 (91%)	51 (81%)	0.052	21 (91%)	116 (87%)	0.771	59 (89%)	78 (86%)	0.495	50 (93%)	87 (84%)	0.147
BMI, kg/m²	22 (15–30)	24 (17–32)	0.103	22 (15–30)	24 (17–32)	0.388	22 (17–32)	23 (15–30)	0.297	23 (15–30)	23 (17–32)	0.645
AST level, IU/L > 40	33 (35%)	20 (32%)	0.663	6 (26%)	47 (35%)	0.400	22 (33%)	31 (34%)	0.924	16 (30%)	37 (36%)	0.428
ALT level, IU/L > 35	49 (52%)	28 (44%)	0.345	9 (39%)	68 (51%)	0.303	33 (50%)	44 (48%)	0.838	24 (44%)	53 (51%)	0.404
AST/ALT	0.890 (0.36–3.50)	1.055 (0.52–2.61)	0.143	0.89 (0.36–3.50)	1.055 (0.52–2.61)	0.214	0.92 (0.36–3.50)	0.95 (0.46–2.89)	0.731	0.935 (0.46–2.89)	0.94 (0.36–3.50)	0.694
TBIL, μmol/L > 17	22 (23%)	22 (35%)	0.115	5 (22%)	39 (29%)	0.467	15 (23%)	29 (32%)	0.208	15 (28%)	29 (28%)	0.960
HBV DNA, × 10⁵ IU/mL	0.016 (0–1300)	0.094 (0–109)	0.204	0.025 (0–1300)	0.096 (0–109)	0.777	0.036 (0–53.80)	0.046 (0–1300)	0.497	0.060 (0–109)	0.037 (0–1300)	0.957
PT, s > 13	75 (80%)	51 (81%)	0.857	19 (83%)	107 (80%)	0.981	50 (76%)	76 (84%)	0.228	46 (85%)	80 (78%)	0.261
AFP, ng/mL > 400	25 (27%)	30 (48%)	0.007	7 (30%)	48 (36%)	0.617	20 (30%)	35 (38%)	0.290	15 (28%)	40 (39%)	0.168
NLR > 2.8	20 (21%)	14 (22%)	0.888	6 (26%)	28 (21%)	0.776	8 (12%)	26 (29%)	0.014	15 (28%)	19 (18%)	0.178
Platelets, 100 × 10⁹/L	162 (33–377)	172 (30–362)	0.916	161 (33–356)	168 (30–377)	0.300	169 (33–373)	165 (30–373)	0.880	158 (47–377)	175 (30–373)	0.666
Albumin, g/L > 35	81 (86%)	60 (95%)	0.066	20 (87%)	121 (90%)	0.907	58 (88%)	83 (91%)	0.496	47 (87%)	94 (91%)	0.406
Number of tumors Single	82 (87%)	52 (83%)	0.415	22 (96%)	112 (84%)	0.233	57 (86%)	77 (85%)	0.760	48 (89%)	86 (83%)	0.364
Tumor size, mm	38 (14–114)	38 (15–133)	0.422	37.5 (14–114)	38 (15–133)	0.251	43 (9–114)	36 (14–133)	0.092	37.5 (14–133)	38.5 (14–114)	0.278
Tumor size group, mm < 50	65 (69%)	46 (73%)	0.602	16 (70%)	95 (71%)	0.897	42 (64%)	69 (76%)	0.098	42 (78%)	69 (67%)	0.168
Child–Pugh I	89 (95%)	62 (98%)	0.441	22 (96%)	129 (96%)	0.889	63 (95%)	88 (97%)	1.000	52 (96%)	99 (96%)	1.000
Differentiation Well	38 (40%)	2 (2%)	< 0.001	15 (65%)	25 (19%)	< 0.001	20 (30%)	20 (22%)	0.237	22 (41%)	18 (17%)	0.001
Moderate + poor	56 (60%)	61 (98%)		8 (35%)	109 (81%)		46 (70%)	71 (78%)		32 (59%)	85 (83%)	
Capsule Present	69 (73%)	43 (68%)	0.484	17 (74%)	95 (71%)	0.767	52 (79%)	60 (66%)	0.079	40 (74%)	72 (70%)	0.583
Microvascular invasion Present	35 (37%)	32 (51%)	0.092	6 (26%)	61 (46%)	0.082	31 (47%)	36 (40%)	0.354	16 (30%)	51 (50%)	0.017

Data are continuous variables, reported as the mean ± standard deviation (SD) or as the median and range and were compared using two-sample t tests or nonparametric Mann–Whitney tests

Data are categorical variables, presented as numbers of patients with percentages in parentheses and were compared using the chi-square test or Fisher's exact test

AST aspartate aminotransferase, ALT alanine aminotransferase, TBIL total bilirubin, HBV hepatitis B virus, PT prothrombin time
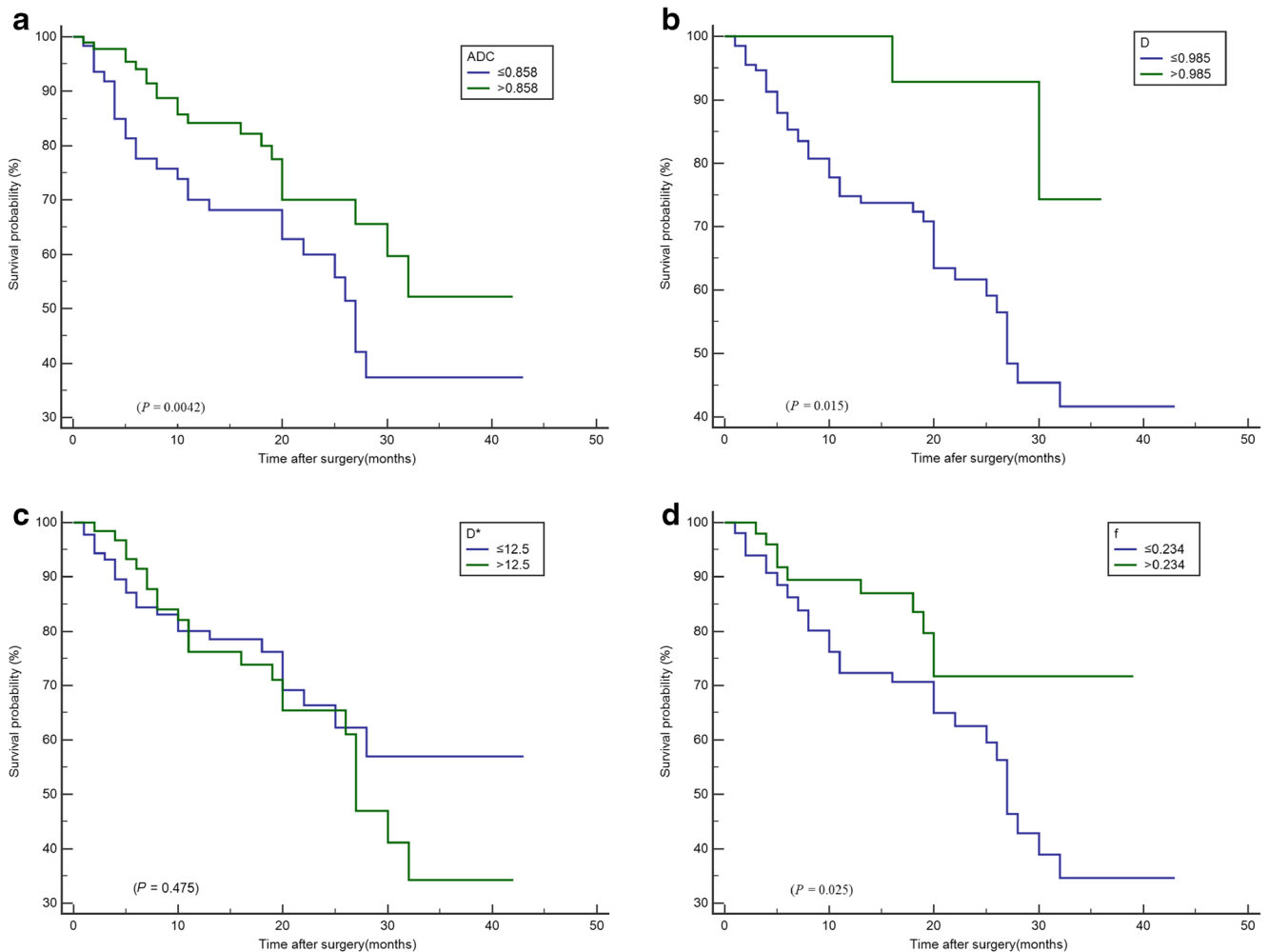
Fig. 2 Comparison of recurrence rates according to the cutoff values of the IVIM values. The Kaplan–Meier analysis shows that the survival time was higher in patients with ADC values $> 0.858 \times 10^{-3}$ mm^2/s than in patients with ADC values $\leq 0.858 \times 10^{-3}$ mm^2/s (a), that the survival time was higher in patients with D values $> 0.985 \times 10^{-3}$ mm^2/s than in patients with D values $\leq 0.985 \times 10^{-3}$ mm^2/s (b), that the survival times were equivalent in patients with D^* values $> 12.5 \times 10^{-3}$ mm^2/s and in patients with ADC values $\leq 12.5 \times 10^{-3}$ mm^2/s (c), and that the survival time was lower in patients with f values $\leq 23.4\%$ than in patients with f values $> 23.4\%$ (d). IVIM, intravoxel incoherent motion; ADC, apparent diffusion coefficient; HCC, hepatocellular carcinoma

Comparison of preoperative characteristics of patients with and without HCC recurrence

A comparison of patients with and without HCC recurrence is presented in supplementary material 1.

Prediction of HCC recurrence

The Kaplan–Meier method and log-rank test revealed that patients with ADC values $\leq 0.858 \times 10^{-3}$ mm^2/s, D values $\leq 0.985 \times 10^{-3}$ mm^2/s, and f values $\leq 23.4\%$ had shorter recurrence-free survival times ($p = 0.015$, $p = 0.042$, and $p = 0.025$, respectively; Fig. 2). D^* was not significantly related to recurrence-free survival ($p = 0.475$; Fig. 2). The univariate Cox proportional hazards model showed that age > 60 years ($p = 0.024$), aspartate aminotransferase > 40 U/L ($p = 0.017$), AFP > 400 mg/dL ($p = 0.014$), ADC values $> 0.858 \times 10^{-3}$ mm^2/s ($p = 0.048$), D values $> 0.985 \times 10^{-3}$ mm^2/s ($p = 0.030$), and f values $> 23.4\%$ ($p = 0.031$) were significant factors for recurrence. The multivariate Cox proportional hazards model revealed that among these factors, age (HR, 0.328; CI, 0.117–0.920, $p = 0.034$), AFP level (HR, 2.079; CI, 1.168–3.701, $p = 0.013$), and D (HR, 0.190; CI, 0.046–0.794, $p = 0.023$) were significant risk factors associated with tumor recurrence after hepatic resection (Table 4). The accuracy based on age and AFP alone was 67.5%, whereas accuracy based on age, AFP, and D value combined was 73.8%. Additional ROC analysis showed that the area under the curve (AUC) of the obtained Cox regression model was improved from 0.68 for the combination of AFP and age to 0.724 for the combination of AFP, age, and D (Fig. 3).

Table 4 Univariate and multivariate analysis of the factors related to recurrence

Characteristics	Univariate			Multivariate			
	B	HR	p value	B	HR	95% CI	p value
Age (> 60 years)	− 1.185	0.306	0.024	− 1.116	0.328	0.117–0.920	0.034
AFP (> 400 mg/dL)	0.721	2.056	0.014	0.732	2.079	1.168–3.701	0.013
ADC (> 0.858×10^{-3} mm^2/s)	− 0.582	0.559	0.048	–	–	–	–
D (> 0.985×10^{-3} mm^2/s)	− 1.570	0.723	0.030	− 1.658	0.190	0.046–0.794	0.023
D* (> 12.5×10^{-3} mm^2/s)	0.206	1.228	0.481	–	–	–	–
f (> 23.4%)	− 0.769	0.464	0.031	–	–	–	–

The multivariate model was adjusted for age at recruitment (> 60 or ≤ 60 years), AFP (> 400 or ≤ 400 mg/dL), AST (> 40 or ≤ 40 IU/L), ALT (> 35 or ≤ 35 IU/L), albumin (> 35 or ≤ 35 g/L), TBIL (> 17 or ≤ 17 μmol/L), PT (> 13 or ≤ 13 s), PLT (> 100 or ≤ 100/L), NLR (> 2.8 or ≤ 2.8), Child–Pugh (I or II), size (> 5 or ≤ 5 cm), number (single or multiple), histological differentiation (well or (moderate + poor)), microvascular invasion (present or absent), capsule (present or absent), ADC (> 0.858 or ≤ 0.858×10^{-3} mm^2/s), D (> 0.985 or ≤ 0.985×10^{-3} mm^2/s), D* (> 12.5 or ≤ 12.5×10^{-3} mm^2/s), and f (> 23.4% or ≤ 23.4%)

AFP α-fetoprotein, *ADC* apparent diffusion coefficient, *AST* aspartate aminotransferase, *ALT* alanine aminotransferase, *TBIL* total bilirubin, *PT* prothrombin time, *PLT* platelet count, *NLR* neutrophil to lymphocyte ratio

Discussion

Our results demonstrated that HCC lesions with lower ADC, D, and f values tended to have poorer histologic differentiation and that lower f values in particular are associated with a higher incidence of microvascular invasion. More pertinently, we showed that patients with lower ADC, D, and f values tend to have a higher incidence of HCC recurrence. Our results also showed that D, along with age and serum AFP levels, is an independent risk factor for HCC recurrence after hepatic resection for HBV-related HCC. When combined with age and AFP levels, D, as derived from IVIM model, can further improve predictions regarding tumor recurrence (Figs. 4 and 5).

Numerous studies have looked to evaluate radiologic features as markers to predict HCC recurrence. Previous studies have shown that tumor hypointensity on Gd-EOB-DTPA-enhanced HBP images may be a useful imaging biomarker to predict poor prognosis in patients with HCC after surgical resection [11, 34]. However, whereas the sensitivity of lesion hypointensity on HBP images was high, the specificity was relatively low potentially limiting its value as a preoperative marker for predicting tumor recurrence. In another study, Lee et al [7] reported that the combination of two or three imaging features (i.e., tumor size, non-smooth tumor margins, and peritumoral enhancement) was indicative of higher rates of early recurrence in patients with a single HCC. In Asia, HBV infection is the predominant etiology of HCC [35], and the mechanisms underlying the related hepatocarcinogenesis, as well as tumor factors and prognosis of HBV-related HCC patients, are different from those caused by other non-viral etiologies [36, 37]. Quantitative biomarkers that can predict tumor recurrence after hepatectomy in patients with HBV-related HCC remain unknown.

In our study, we found that tumor recurrence was more frequent in HCC patients with lower ADC values (≤ 0.858×10^{-3} mm^2/s), D values (≤ 0.985×10^{-3} mm^2/s), and f values (≤ 23.4%) derived from IVIM DWI. In support of our findings, Muhi et al [14] found that the recurrence rate was increased and the 3- and 5-year survival rates significantly decreased in HCC patients with ADC values ≤ 0.898×10^{-3} mm^2/s, i.e., at an ADC cutoff very similar to that in our study.
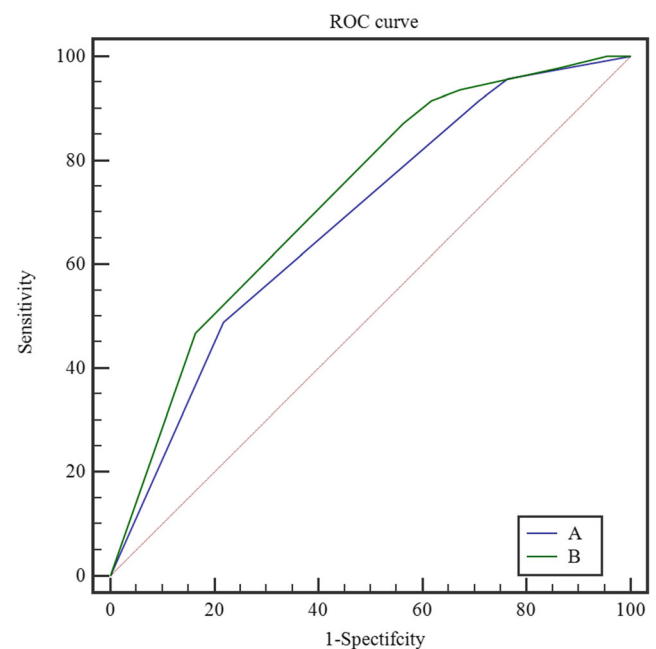
Fig. 3 Comparison of the ROC curve analyses of the obtained Cox regression model for the combination of AFP and age alone (A) and for the combination of D, AFP, and age (B)
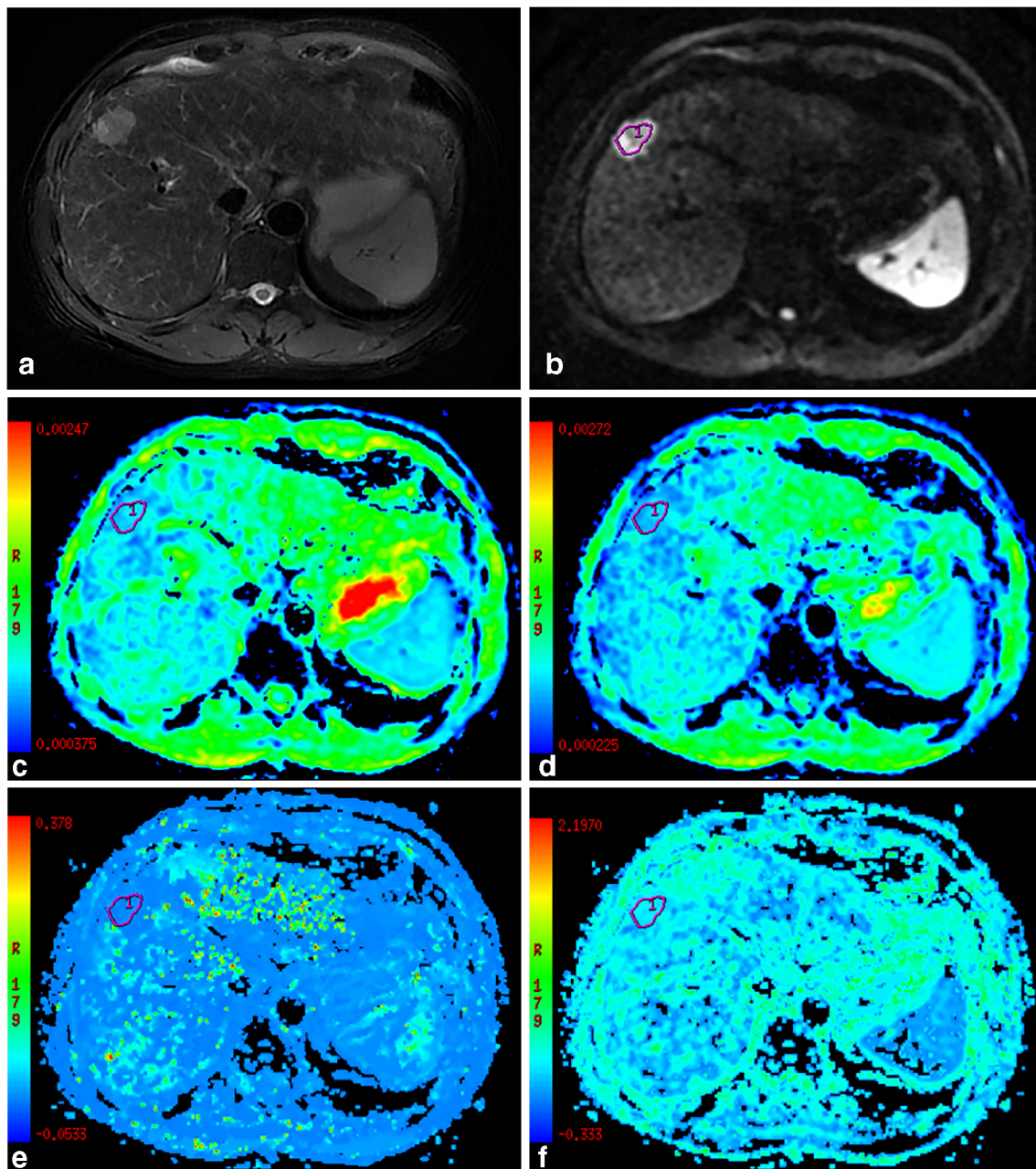
Fig. 4 A patient with HCC that was treated with curative resection. The lesion had a low D value. Tumor recurrence occurred 4.67 months after surgery. **a** Fat-suppressed axial T2WI showing a focal liver lesion with an obvious hyperintense signal. **b** Axial diffusion-weighted image with a $b = 800$ s/mm^2 shows a hyperintense focal liver lesion. **c–f** ADC, D, $D*$, and f pseudocolorized maps showing that the mean ADC, D, $D*$, and f values of the tumor were 0.817×10^{-3} mm^2/s, 0.709×10^{-3} mm^2/s, 5.78×10^{-3} mm^2/s, and 25%, respectively. ADC, apparent diffusion coefficient

It is established that histologic differentiation is one of the most important predictive factors of recurrence and survival after liver transplantation and hepatic resection [24, 38, 39]. A possible reason for the higher recurrence rate in patients with lower tumor ADC, D, and f values in our study may therefore be the greater proportion of poorly differentiated HCC lesions in our population. It is likely that the increased cellular density and decreased blood supply associated with poorly differentiated HCC result in decreased ADC, D and f values [20, 40, 41].

Our results revealed that HCCs with microvascular invasion, which is related to a 4.4-fold increase in the risk of tumor recurrence [42, 43], tend to have low f values. This may be another explanation for the higher recurrence rate of HCCs in patients with lower f values. The reason for which lower f values tend to be observed in HCCs with microvascular invasion is not completely understood but is most likely related to a decreased hemodynamic perfusion in HCC. Unfortunately, the bi-exponential IVIM model for DWI cannot explain the
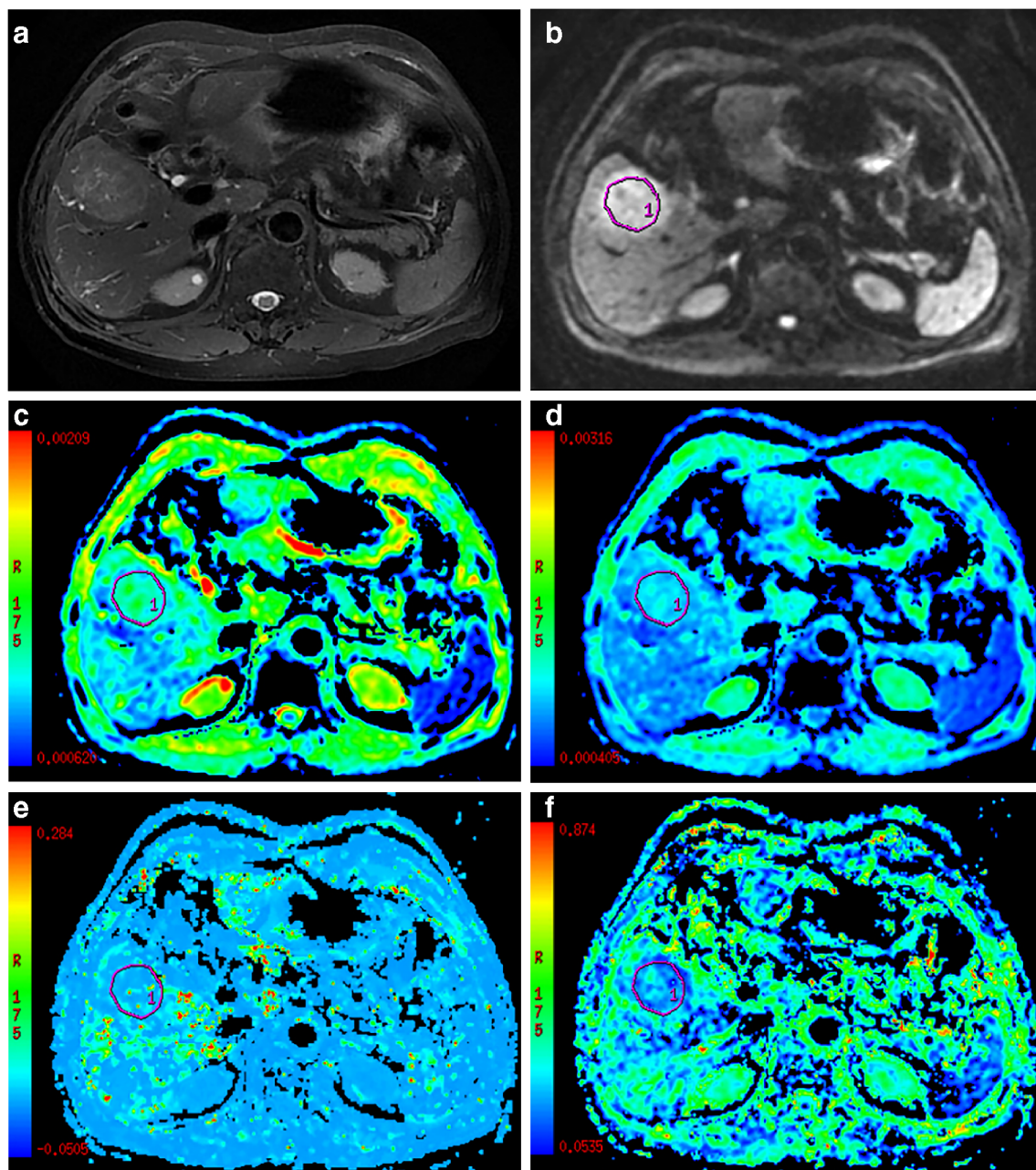
Fig. 5 A patient with HCC treated with curative resection without recurrence during a follow-up period of 19.75 months. The lesion had a high D value. **a** Fat-suppressed axial T2WI showing a focal liver lesion with obvious hyperintense signal. **b** Axial diffusion-weighted image with a $b = 800$ s/mm^2 shows a hyperintense focal liver lesion. **c–f** ADC, D, D^*, and f pseudocolorized maps show that the mean ADC, D, D^*, and f values of the tumor were 1.09×10^{-3} mm^2/s, 0.994×10^{-3} mm^2/s, 20.8×10^{-3} mm^2/s, and 18.3%, respectively. ADC, apparent diffusion coefficient

differential T2s in the model compartments, which results in an overestimation of pseudodiffusion fraction f in the liver [44, 45]. Therefore, the observed changes in pseudodiffusion fraction f in a clinical setting should be interpreted with caution. In our study, there was no correlation between the D^* values and tumor recurrence which may have been due to the poor reproducibility of D^*. Similar to our results, a previous study also demonstrated poor measurement reproducibility for D^* [46, 47]. Heterogeneity of HCC could be one of the

contributing factors to the poor measurement reproducibility of D^* [46]. In addition, respiratory-triggering techniques, distribution of b values, and bi-exponential fitting problems may be other contributing factors [47–50]. Hence, further technical improvements are needed to strengthen the robustness of D^*.

Whereas low ADC, D, and f values were associated with tumor recurrence, D, along with age and serum AFP levels, was found to be an independent risk factor for tumor recurrence after hepatic resection for HBV-related HCCs. The

reason why D is an independent risk factor for predicting HCC recurrence might be that increased cellular density and increased nuclear-to-cytoplasmic ratio would be more prominent pathophysiologic phenomena than decreased blood perfusion in the recurrence of HCC [20]. Importantly, D values can be calculated from DWI at two b values. Therefore, a shorter DWI acquisition tailored to derive D alone may be a more practical and time-saving approach in clinical practice. Further research is needed to investigate this possibility.

In addition to MRI features, clinical markers can be potentially useful to preoperatively predict prognosis after curative resection of HCCs. In our study, elevated preoperative serum AFP level was associated with HCC recurrence. This finding was consistent with those of previous studies [51, 52]. However, An et al [8] reported that AFP was not a significant predictor of recurrence. This discrepancy in observations may be attributed to the heterogeneity of the patient populations evaluated. In addition, younger age was also associated with tumor recurrence. The reasons for the poorer prognosis of younger HCC patients may be due to their having a more advanced disease stage at diagnosis, a higher number of tumor nodules, and a more biologically aggressive tumor [53, 54].

In our study, the addition of D to AFP and age improved the preoperative predictive performance of HCC recurrence. An integrated model derived from these variables revealed an AUC of 0.724 for prediction of the risk of tumor recurrence. Previous studies reported that elevated serum AFP levels and younger age were associated with HCC recurrence [51–53]. An et al [8] reported that four MRI features, namely, rim enhancement, peritumoral parenchymal enhancement in the arterial phase, satellite nodules, and tumor size, were independently associated with early recurrence only in patients with a single tumor. Unlike these morphological features, quantitative IVIM values derived from DWI do not depend on contrast agents and could be used in patients with liver or renal insufficiency.

There were several limitations to our study. First, we only focused on HBV-related HCCs. Diffusion and blood perfusion effects may be different in HCCs caused by other etiologies. The cutoff values derived from IVIM warrant validation in other HCC populations with different etiologies for chronic liver diseases. Second, we measured IVIM parameters in the target tumor with the longest cross-section. However, single-slice ROI methods may not reflect the overall characteristic of the tumor. It is known that intra-tumor heterogeneity can be better captured by analyzing the entire tumor volume. Future work should therefore focus on the whole tumor volume rather than using one-section ROI methods. Third, histopathological proof was absent in 34 of 47 recurrent tumors. Last, the follow-up time was relatively short. Future work should prolong the follow-up period to better evaluate the long-term survival outcome and the role of IVIM parameters in predicting HCC recurrence.

In conclusion, our results suggest that lower ADC, D, and f values are associated with increased HCC recurrence in patients with HCC after hepatectomy. The D value may be a useful biomarker for preoperative prediction of recurrence after hepatectomy in patients with HBV-related HCC. When combined with age and AFP levels, D values can further improve the performance of predicting tumor recurrence. Patients with low D values, younger age, and high AFP levels may need more regular follow-up after curative hepatectomy to detect possible recurrence. Therefore, a shorter DWI acquisition tailored to derive D alone may be more practical and time-saving in clinical practice.

Compliance with ethical standards

Guarantor The scientific guarantor of this publication is Jin Wang.

Conflict of interest The authors of this manuscript declare no relationships with any companies whose products or services may be related to the subject matter of the article.

Statistics and biometry No complex statistical methods were necessary for this paper.

Informed consent Written informed consent was waived by the Institutional Review Board.

Ethical approval Institutional Review Board approval was obtained.

Methodology
• retrospective
• diagnostic or prognostic study
• performed at one institution

References

1. Bruix J, Sherman M (2011) Management of hepatocellular carcinoma: an update. Hepatology 53:1020–1022
2. Torre LA, Bray F, Siegel RL, Ferlay J, Lortet-Tieulent J, Jemal A (2015) Global cancer statistics, 2012. CA Cancer J Clin 65:87–108
3. Portolani N, Coniglio A, Ghidoni S et al (2006) Early and late recurrence after liver resection for hepatocellular carcinoma. Ann Surg 243:229–235
4. Chong CC, Lee KF, Ip PC et al (2012) Pre-operative predictors of post-hepatectomy recurrence of hepatocellular carcinoma: can we predict earlier? Surgeon 10:260–266
5. Cheng Z, Yang P, Qu S et al (2015) Risk factors and management for early and late intrahepatic recurrence of solitary hepatocellular carcinoma after curative resection. HPB (Oxford) 17:422–427
6. Li T, Qin LX, Gong X et al (2014) Clinical characteristics, outcome, and risk factors for early and late intrahepatic recurrence of female

patients after curative resection of hepatocellular carcinoma. Surgery 156:651–660

7. Lee S, Kim SH, Lee JE, Sinn DH, Park CK (2017) Preoperative gadoxetic acid-enhanced MRI for predicting microvascular invasion in patients with single hepatocellular carcinoma. J Hepatol 67:526–534

8. An C, Kim DW, Park YN, Chung YE, Rhee H, Kim MJ (2015) Single hepatocellular carcinoma: preoperative MR imaging to predict early recurrence after curative resection. Radiology 276:433–443

9. Ariizumi S, Kitagawa K, Kotera Y et al (2011) A non-smooth tumor margin in the hepatobiliary phase of gadoxetic acid disodium (Gd-EOB-DTPA)-enhanced magnetic resonance imaging predicts microscopic portal vein invasion, intrahepatic metastasis, and early recurrence after hepatectomy in patients with hepatocellular carcinoma. J Hepatobiliary Pancreat Sci 18:575–585

10. Ahn SY, Lee JM, Joo I et al (2015) Prediction of microvascular invasion of hepatocellular carcinoma using gadoxetic acid-enhanced MR and (18)F-FDG PET/CT. Abdom Imaging 40:843–851

11. Choi JW, Lee JM, Kim SJ et al (2013) Hepatocellular carcinoma: imaging patterns on gadoxetic acid-enhanced MR images and their value as an imaging biomarker. Radiology 267:776–786

12. Toyoda H, Kumada T, Tada T et al (2013) Non-hypervascular hypointense nodules detected by Gd-EOB-DTPA-enhanced MRI are a risk factor for recurrence of HCC after hepatectomy. J Hepatol 58:1174–1180

13. Barral M, Taouli B, Guiu B et al (2015) Diffusion-weighted MR imaging of the pancreas: current status and recommendations. Radiology 274:45–63

14. Muhi A, Ichikawa T, Motosugi U et al (2013) Diffusion-weighted imaging of hepatocellular carcinoma for predicting early recurrence and survival after hepatectomy. Hepatol Int 7:662–668

15. Xu P, Zeng M, Liu K, Shan Y, Xu C, Lin J (2014) Microvascular invasion in small hepatocellular carcinoma: is it predictable with preoperative diffusion-weighted imaging? J Gastroenterol Hepatol 29:330–336

16. Suh YJ, Kim MJ, Choi JY, Park MS, Kim KW (2012) Preoperative prediction of the microvascular invasion of hepatocellular carcinoma with diffusion-weighted imaging. Liver Transpl 18:1171–1178

17. Luciani A, Vignaud A, Cavet M et al (2008) Liver cirrhosis: intravoxel incoherent motion MR imaging–pilot study. Radiology 249:891–899

18. Yoon JH, Lee JM, Yu MH, Kiefer B, Han JK, Choi BI (2014) Evaluation of hepatic focal lesions using diffusion-weighted MR imaging: comparison of apparent diffusion coefficient and intravoxel incoherent motion-derived parameters. J Magn Reson Imaging 39:276–285

19. Le Bihan D, Breton E, Lallemand D, Aubin ML, Vignaud J, Laval-Jeantet M (1988) Separation of diffusion and perfusion in intravoxel incoherent motion MR imaging. Radiology 168:497–505

20. Woo S, Lee JM, Yoon JH, Joo I, Han JK, Choi BI (2014) Intravoxel incoherent motion diffusion-weighted MR imaging of hepatocellular carcinoma: correlation with enhancement degree and histologic grade. Radiology 270:758–767

21. Roayaie S, Jibara G, Taouli B, Schwartz M (2013) Resection of hepatocellular carcinoma with macroscopic vascular invasion. Ann Surg Oncol 20:3754–3760

22. Gao F, Zhu HK, Zhu YB et al (2016) Predictive value of tumor markers in patients with recurrent hepatocellular carcinoma in different vascular invasion pattern. Hepatobiliary Pancreat Dis Int 15:371–377

23. Shah SA, Cleary SP, Wei AC et al (2007) Recurrence after liver resection for hepatocellular carcinoma: risk factors, treatment, and outcomes. Surgery 141:330–339

24. Lauwers GY, Terris B, Balis UJ et al (2002) Prognostic histologic indicators of curatively resected hepatocellular carcinomas: a multi-institutional analysis of 425 patients with definition of a histologic prognostic index. Am J Surg Pathol 26:25–34

25. Verslype C, Rosmorduc O, Rougier P (2012) Hepatocellular carcinoma: ESMO-ESDO Clinical Practice Guidelines for diagnosis, treatment and follow-up. Ann Oncol 23 Suppl 7:vii41–48

26. Bruix J, Sherman M (2011) Management of hepatocellular carcinoma: an update. Hepatology 53:1020–1022

27. Wurnig MC, Donati OF, Ulbrich E et al (2015) Systematic analysis of the intravoxel incoherent motion threshold separating perfusion and diffusion effects: proposal of a standardized algorithm. Magn Reson Med 74:1414–1422

28. Sigmund EE, Vivier PH, Sui D et al (2012) Intravoxel incoherent motion and diffusion-tensor imaging in renal tissue under hydration and furosemide flow challenges. Radiology 263:758–769

29. Patel J, Sigmund EE, Rusinek H, Oei M, Babb JS, Taouli B (2010) Diagnosis of cirrhosis with intravoxel incoherent motion diffusion MRI and dynamic contrast-enhanced MRI alone and in combination: preliminary experience. J Magn Reson Imaging 31:589–600

30. Kim SY, Lee SS, Byun JH et al (2010) Malignant hepatic tumors: short-term reproducibility of apparent diffusion coefficients with breath-hold and respiratory-triggered diffusion-weighted MR imaging. Radiology 255:815–823

31. American College of Radiology (2017) Liver imaging reporting and data system. American College of Radiology. https://www.acr.org/Quality-Safety/Resources/LIRADS. Accessed 1 Jul 2017

32. Kundel HL, Polansky M (2003) Measurement of observer agreement. Radiology 228:303–308

33. Nougaret S, Vargas HA, Lakhman Y et al (2016) Intravoxel incoherent motion-derived histogram metrics for assessment of response after combined chemotherapy and radiation therapy in rectal cancer: initial experience and comparison between single-section and volumetric analyses. Radiology 280:446–454

34. Kitao A, Matsui O, Yoneda N et al (2012) Hypervascular hepatocellular carcinoma: correlation between biologic features and signal intensity on gadoxetic acid-enhanced MR images. Radiology 265:780–789

35. de Martel C, Maucort-Boulch D, Plummer M, Franceschi S (2015) World-wide relative contribution of hepatitis B and C viruses in hepatocellular carcinoma. Hepatology 62:1190–1200

36. Kao WY, Su CW, Chau GY, Lui WY, Wu CW, Wu JC (2011) A comparison of prognosis between patients with hepatitis B and C virus-related hepatocellular carcinoma undergoing resection surgery. World J Surg 35:858–867

37. Zhou Y, Si X, Wu L, Su X, Li B, Zhang Z (2011) Influence of viral hepatitis status on prognosis in patients undergoing hepatic resection for hepatocellular carcinoma: a meta-analysis of observational studies. World J Surg Oncol 9:108

38. Jonas S, Bechstein WO, Steinmüller T et al (2001) Vascular invasion and histopathologic grading determine outcome after liver transplantation for hepatocellular carcinoma in cirrhosis. Hepatology 33:1080–1086

39. Kim SU, Jung KS, Lee S et al (2014) Histological subclassification of cirrhosis can predict recurrence after curative resection of hepatocellular carcinoma. Liver Int 34:1008–1017

40. Granata V, Fusco R, Catalano O et al (2016) Intravoxel incoherent motion (IVIM) in diffusion-weighted imaging (DWI) for hepatocellular carcinoma: correlation with histologic grade. Oncotarget 7:79357–79364

41. Nakanishi M, Chuma M, Hige S et al (2012) Relationship between diffusion-weighted magnetic resonance imaging and histological tumor grading of hepatocellular carcinoma. Ann Surg Oncol 19:1302–1309

42. Renzulli M, Brocchi S, Cucchetti A et al (2016) Can current pre-operative imaging be used to detect microvascular invasion of hepatocellular carcinoma? Radiology 279:432–442

43. Colecchia A, Schiumerini R, Cucchetti A et al (2014) Prognostic factors for hepatocellular carcinoma recurrence. World J Gastroenterol 20:5935–5950

44. Jerome NP, d'Arcy JA, Feiweier T et al (2016) Extended T2-IVIM model for correction of TE dependence of pseudo-diffusion volume fraction in clinical diffusion-weighted magnetic resonance imaging. Phys Med Biol 61:N667–N680

45. Lemke A, Laun FB, Simon D, Stieltjes B, Schad LR (2010) An in vivo verification of the intravoxel incoherent motion effect in diffusion-weighted imaging of the abdomen. Magn Reson Med 64:1580–1585

46. Andreou A, Koh DM, Collins DJ et al (2013) Measurement reproducibility of perfusion fraction and pseudodiffusion coefficient derived by intravoxel incoherent motion diffusion-weighted MR imaging in normal liver and metastases. Eur Radiol 23:428–434

47. Jerome NP, Miyazaki K, Collins DJ et al (2017) Repeatability of derived parameters from histograms following non-Gaussian diffusion modelling of diffusion-weighted imaging in a paediatric oncological cohort. Eur Radiol 27:345–353

48. Cohen AD, Schieke MC, Hohenwalter MD, Schmainda KM (2015) The effect of low b-values on the intravoxel incoherent motion derived pseudodiffusion parameter in liver. Magn Reson Med 73: 306–311

49. Dyvorne H, Jajamovich G, Kakite S, Kuehn B, Taouli B (2014) Intravoxel incoherent motion diffusion imaging of the liver: optimal b-value subsampling and impact on parameter precision and reproducibility. Eur J Radiol 83:2109–2113

50. Kakite S, Dyvorne H, Besa C et al (2015) Hepatocellular carcinoma: short-term reproducibility of apparent diffusion coefficient and intravoxel incoherent motion parameters at 3.0T. J Magn Reson Imaging 41:149–156

51. Xia Y, Yan ZL, Xi T et al (2012) A case-control study of correlation between preoperative serum AFP and recurrence of hepatocellular carcinoma after curative hepatectomy. Hepatogastroenterology 59: 2248–2254

52. Ma WJ, Wang HY, Teng LS (2013) Correlation analysis of preoperative serum alpha-fetoprotein (AFP) level and prognosis of hepatocellular carcinoma (HCC) after hepatectomy. World J Surg Oncol 11:212

53. Cho SJ, Yoon JH, Hwang SS, Lee HS (2007) Do young hepatocellular carcinoma patients with relatively good liver function have poorer outcomes than elderly patients? J Gastroenterol Hepatol 22:1226–1231

54. Wai CT, Woon WA, Tan YM, Lee KH, Tan KC (2012) Younger age and presence of macrovascular invasion were independent significant factors associated with poor disease-free survival in hepatocellular carcinoma patients undergoing living donor liver transplantation. Transplant Proc 44:516–519